Hindawi
International Journal of Geophysics
Volume 2023, Article ID 4181389, 13 pages
https://doi.org/10.1155/2023/4181389

Research Article

Koudougou (Burkina Faso, Africa), GPS-TEC Response to Recurrent Geomagnetic Storms during Solar Cycle 24 Declining Phase

Saguedo Sawadogo, Doua Allain Gnabahou, Sibri Alphonse Sandwidi, and Frédéric Ouattara

Research Laboratory in Energetics and Space Weather (LAREME), University Norbert ZONGO (UNZ), BP 376 Koudougou, Burkina Faso

Correspondence should be addressed to Doua Allain Gnabahou; gnabahou@yahoo.fr

Received 7 February 2023; Revised 22 March 2023; Accepted 27 March 2023; Published 10 April 2023

Academic Editor: Angelo De Santis

In this paper, we presented the effect of moderate geomagnetic storms on the TEC variation at the Koudougou station (Geo Lat 12° 15′ N; Geo Long: -2° 20′ E) in Burkina Faso (Africa) during the descending phase of solar cycle 24. For this purpose, four moderate geomagnetic storms without storm sudden commencement (SSC) or sudden impulse (SI) that occurred on May 13, 2015 (Dst: -76 nT), June 08, 2015 (Dst: -73 nT), September 11, 2015 (Dst: -80 nT), and May 08-09, 2016 (Dst: -88nT), were considered. These moderate storms were found to be associated with transients induced by fast solar winds. At the Koudougou station, TEC variation shows a positive response to the different moderate geomagnetic storms studied, with increases of order of 2-21 TECU around 1300-1500 UT except for September 11, 2015, TEC variation which shows sometimes negative responses at a few hours (mainly at night). TEC increases observed are a function of geomagnetic parameter (magnitude and polarity) variation. Storm-induced electric field and neutral winds are the main drivers of TEC changes observed during the selected geomagnetic storms. In addition, it was found that the TEC peak on storm day behaves differently compared to the days before and after the storm depending on whether Dst is positive or negative before southward inversion. Indeed, a TEC small peak relative to the days before and after the storm is observed when Dst is negative before southward inversion, and a larger peak occurs in the opposite case. The reasons for these differences are not investigated in this paper.

1. Introduction

Sun is the solar system main source of energy. It continuously releases energy into interplanetary space in electromagnetic radiation form and charged particles that are responsible for the Sun-magnetosphere-ionosphere dynamics [1]. A variety of physical phenomena are associated with space weather, including geomagnetic storms, geomagnetic activity, ionospheric disturbances, flickers, auroras, and Earth-induced telluric currents [2]. Geomagnetic storms result from solar wind's interaction energy transferred to the Earth's magnetosphere through magnetic reconnection [3]. They are generally caused by coronal mass ejections (CMEs) from the Sun [4–6] and corotating interaction regions (CIRs) created by the interaction between slow and fast solar winds from coronal holes [7–9].

According to Perreault and Akasofu [10], geomagnetic storms can be defined as magnetosphere's response to intense solar wind flow impact in which intensity and direction of magnetic field vary in a complex manner. Conventionally, several geomagnetic indices are used to assess the strength of a geomagnetic storm. However, for equatorial regions, the most commonly used indices are (i) the disturbance storm time (Dst) index [11–13] and (ii) the Kp index which is an integer between 0 and 9 [13–15]. Gonzalez et al. [16] define three classes of geomagnetic storms according to their intensity based on the Dst index: (i) weak storms characterized by $-50\,\mathrm{nT} < \mathrm{Dst} \leq -30\,\mathrm{nT}$, (ii) moderate storms

determined by $-100\,\text{nT} < \text{Dst} \leq -50\,\text{nT}$, and (iii) intense storms with $\text{Dst} \leq -100\,\text{nT}$. Other authors such as Loewe and Prölss [17] even speak of severe storms when $\text{Dst} \leq -200\,\text{nT}$. Here, our study concerns moderate storms.

Geomagnetic storm's main effect on the magnetosphere is the injection of many energetic ions and electrons from the tail, significantly increasing ring current. Depending on whether Earth's magnetosphere reaction time is fast or slow, two types of storms have been detected: (i) sudden storm commencement (SSC) [18–20] and (ii) progressive onset geomagnetic storms [21, 22]. These latter are also called recurrent storms [23–25]. This paper discusses these types of geomagnetic storms during solar cycle 24 descending phase.

Geomagnetic storms can significantly alter ionosphere and have significant negative effects on space and ground systems [26]. During storms, solar wind/magnetosphere coupling leads to increased Joule heating. This results perturbations in the composition, temperature, density, and winds of the upper atmosphere [27–29] that influence aerospace systems and associated human technologies. Examples of activities directly impacted are radio wave propagation, sending signals between satellites and Earth, control of communication and navigation systems, etc. [30, 16]. Therefore, it is important to know ionosphere in more depth and to study its behavior.

In communication and navigation systems' case, one of the ionospheric parameters with a dominant influence on system performance is total electronic content (TEC). GPS signals' range errors are directly proportional to TEC; therefore, any variation in this is a major concern [31]. Thus, several ionospheric models have been developed to better understand these variations. The best known are, for example, Klobuchar model [32], SAMI model [33], NTCM model [34], NeQuick model [35, 36], or IRI (International Reference Ionosphere) model [37].

In the past, many studies have been conducted on storm effects on the ionosphere at high and midlatitudes [38, 39] and low latitudes [40–44]. Pedatella et al. [45] investigated the TEC variation during December 15, 2006, storm over Pacific Ocean region using multi-instrument data. Rama Rao et al. [46] studied the TEC variation at different latitudes over the Indian sectors and geomagnetic storms impact on navigation systems by considering two successive storms that occurred between November 8 and 12, 2004. Kumar et al. [47] reported that electric field induced by the storm can trigger the growth of the Rayleigh-Taylor instability and consequently the development of plasma bubble. Singh et al. [48] studied four intense geomagnetic storm effects on low-latitude TEC during ascending phase of solar cycle 24. An analysis of ionospheric TEC from GPS, GIM, and global ionospheric models during moderate, strong, and extreme geomagnetic storms over the Indian region was done by Reddybattula et al. [49].

However, the complex processes that occur in the upper atmosphere during geomagnetic storms make accurate modeling difficult. Existing models can only provide monthly averages of actual variability, especially during periods of magnetic quiet [27]. Geomagnetic phenomena's complexity makes modeling hard during disturbed period complex, hence interest in studying response of Koudougou station' TEC data during disturbed periods in general and particularly during moderate geomagnetic storms.

Data and analysis method are presented in Section 2. Section 3 concerns results and discussion. Conclusion is presented in Section 4.

2. Data and Analysis

2.1. Data Used. Annual sunspot number (SN) values were used to partition solar cycle into phases. These SN values are available on Sunspot Index and Long-term Solar Observations (SILSO) website at https://www.sidc.be/silso/datafiles. Vertical total electron content (VTEC) data used in this study are from Koudougou GPS station (Geo Lat 12° 15′ N; Geo Long: -2° 20′ E). This is an equatorial station located in West Africa, precisely in the center-west of Burkina Faso. It was installed in November 2008 as part of International Heliophysical Year (IHY) project. The database stores input data for VTEC calculation in RINEX (Receiver Independent Exchange Format) with cadences of 450 seconds.

Solar wind parameters have been used to evaluate Sun's contribution on geomagnetic storms. These parameters are available on the OMNIWeb database (https://omniweb.gsfc.nasa.gov/form/dx1.html). Solar wind parameters such as speed (SSW), temperature (SWPT), and plasma pressure (SWP) as well as magnetic field magnitudes (B_Z component and total magnetic field B_T) were used. Also the data of y component of electric field (IEF Ey) also used in this work are downloadable on the same site.

Geomagnetic indices were used to select geomagnetic activity different days according to existing classes. These indices are available on the International Service of Geomagnetic Indices (ISGI) website (http://isgi.unistra.fr/data_download.php). Indices used in this work are (i) Dst index and (ii) Kp index. Dst index indicates horizontal component's hourly variation of Earth's magnetic field [3]. It is storm intensity indicator but is not a geomagnetic activity's good tracer in usual sense, for which Kp index should be considered instead [50]. Interplanetary index Kp indicates geomagnetic activity's level. It varies between 0 and 9 according to the intensity of terrestrial magnetosphere's disturbance. But Kp on OMNIWeb base has been subject to a special treatment, explained in the OMNIWeb site at https://omniweb.gsfc.nasa.gov/html/ow_data.html.

2.2. Methods of Analysis. In the present study, recurrent geomagnetic storm day's selection was performed using a pixel diagram constructed from Kp OMNI data. Each line represents a Bartels rotation, the double black circles represent SSC dates, and the single black circles represent SI dates. The method was first used by Legrand and Simon [23] with the geomagnetic index values aa for geomagnetic activity day classification. It was then improved by Ouattara and Amory-Mazaudier [24] and a little later by Zerbo et al. [25]. More recently, the authors have appreciated Kp index's reliability compared to the aa index. Kp index combined with other indices such as Dst or SymH is an excellent indicator for

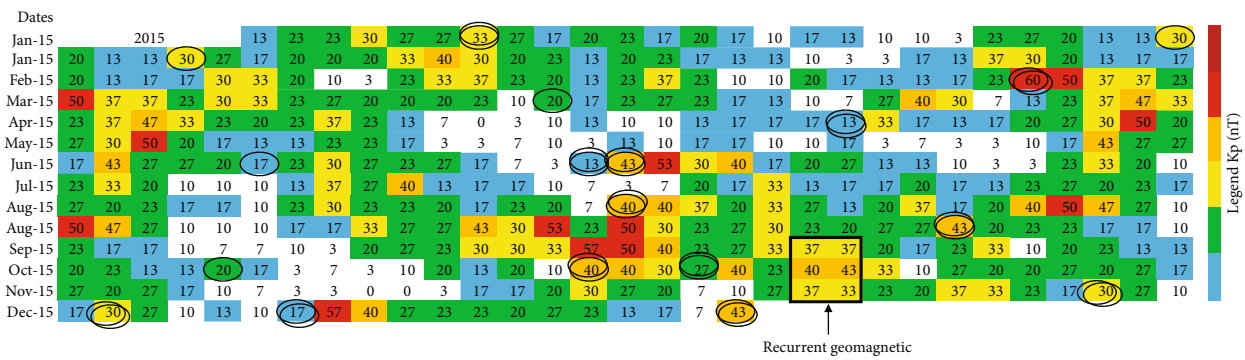

Figure 1: Pixel diagram from 2015. Each line represents a Bartels rotation, the double black circles represent the SSC dates, and the single circles represent the SI.

Table 1: Dst and Kp extreme values during geomagnetic storms and month calm days.

Storm date	Dst_{Min}	Kp_{max}	Quiet days of the month (Kp < 20)
13-05-2015	-76	57	01-05, 07-09, 15-17, and 20-31 (23 days in May 2015)
08-06-2015	-73	60	01-07, 18-20, 26, and 29-30 (13 days in June 2015)
11-09-2015	-80	70	01-03, 24-30 (10 days in September 2015)
08&09-05-2016	-88	63	04-05, 11-13, 18-20, and 22-26 (13 days in May 2016)

geomagnetic activity day selection [51]. It is used for the selection of international calm and disturbed days in the month [52]. Figure 1 shows an example of a pixel diagram constructed using Kp OMNI. Recurrent days are identified by Kp ≥ 30 spanning one or more Bartels rotations without SSC or SI (sudden impulsion).

The moderate storm day selection criteria are (i) $-100\ nT < Dst \leq -50\ nT$, (ii) $SWPT \geq 105\ K$, and (iii) $SSW \geq 500\ km/s$); (iv) day selected must not be preceded by an SSC or SI. Taking these criteria into account, four storms were selected. Table 1 contains the dates of the selected storms and Kp OMNI and Dst indices maximum and minimum values and Dst indices, respectively.

TEC measurements' relative deviation (δTEC) on disturbed days compared to those on calm days is calculated using the following equation:

$$\delta\text{TEC} = \frac{(\text{TEC}_S - \text{TEC}_Q)}{\text{TEC}_Q} \times 100, \quad (1)$$

where TEC_S is TEC for stormy day and TEC_Q is daily average TEC for month quiet days considerate. Sandwidi and Ouattara [53] used this method to study the impact of recurrent events on foF2 critical frequency at Dakar station (Lat: 14.8° N, Long: 342.6° E, Senegal).

3. Results and Discussion

In this section, the TEC variation during moderate recurrent geomagnetic storms whose dates are given in Table 1 is presented. For this study, we have also considered the two close days before and after the storm. Red vertical line on the figures indicates storm actual start. In the TEC curves, event day TEC and calm days' TEC are displayed in black and orange, respectively. The calm day TEC was calculated by averaging the calm day TEC values of the given month.

3.1. TEC Variation from May 11 to May 15, 2015. Variation of Dst index, solar wind speed (SSW), proton pressure (SWP), solar wind proton temperature (SWPT), horizontal component of the interplanetary magnetic field (IMF B_Z), component y of the interplanetary electric field (IEF Ey), and total electron content (TEC) at the Koudougou station from May 11 to 15, 2015, are presented in Figures 2(a)–2(f), respectively. This moderate geomagnetic storm started on May 12, 2015, around 2300 UT. Figure 2(a) shows that Dst index started to turn southward at 0000 UT and reached its minimum value (-76 nT) on 13 May 2015 around 0600 UT (i.e., six hours later). It remained in this direction until 14 May 2015 at 0100 UT when it returned to the normal variation of a calm day. Figures 2(b)–2(d) show an increase in solar wind speed, pressure, and temperature, respectively, just after the storm start commencement. The sudden increase in these solar wind parameters indicates a shock wave arrival [39]. Well before the storm's real commencement, a transient behavior of Dst index is observed where it showed twice a southward polarity, the first one at 0400 UT on 11 May 2015 (-51 nT) and the second one at 1800 UT on 12 May 2015 (-44 nT). Also, a north-south oscillation of B_Z is observed between 11 and 12 May 2015.

The north-south oscillation of Dst index and B_Z on 11-12 May 2015 could be the condition for a succession of substorms [54]. At the Koudougou GPS station, TEC smallest values are observed at 0400 UT with a strong decrease from 2200 UT. These times prevail during night hours at the station, and thus, TEC depression is evident due to opposite polarity of electric field PP and the ambient field. On May 11 and 12, TEC has a remarkable increase between 1100

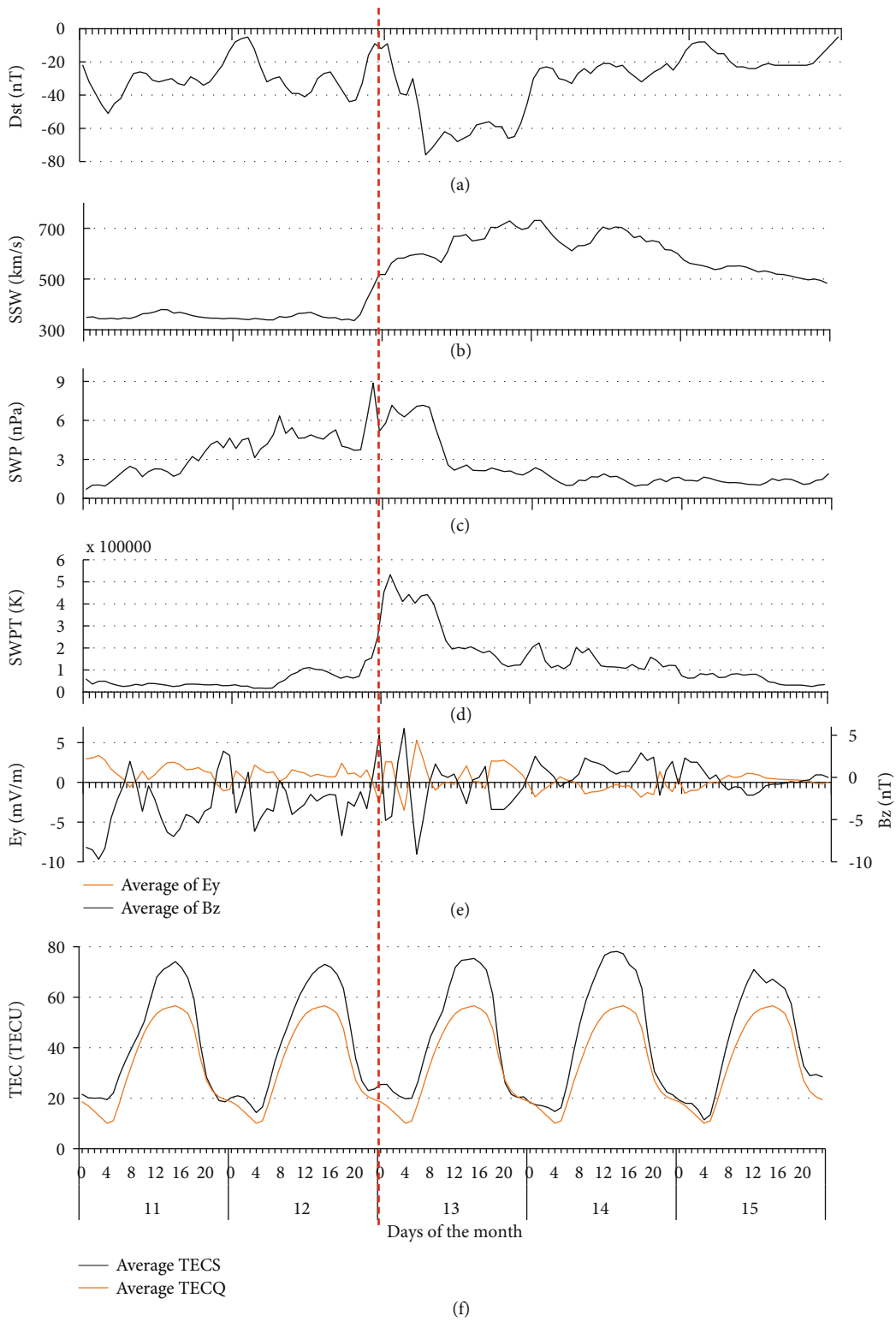

Figure 2: Variation of solar wind parameters and total electron content (TEC) from May 11 to 15, 2015, at the Koudougou GPS station.

UT and 1800 UT with a maximum value of 74.11 TECU and 72.99 TECU, respectively, at 1500 UT (i.e., an increase of 17.5 TECU and 16.38 TECU, respectively). Meanwhile, B_Z has a nonconstant direction and Ey an eastern, almost constant direction, and its value varies between 0.96 and 2.25 mV/m. Fejer et al. [55] pointed out that prompt penetrating electric fields (PPEF) reach the equatorial region only when the IMF B_Z is stable and moving southward. In addition, Huang et al. [56] showed that the efficiency of electric field penetration into the equatorial ionosphere on the day

side is about 10% of the IEF Ey values and will be effective when the IEF Ey varies between 20 and 30 mV/m. Therefore, the daytime-side increase in the TEC of May 11-12, 2015, is not due to the PPEF. However, the cause of the TEC increase could be the substorm effect. Indeed, Wei et al. [57] explained that substorms could cause such an increase in TEC at the equatorial level with a process being faster and more efficient due to the pulses of the equatorial electric field caused by IEF fluctuations or the solar wind dynamic pressure.

Dst variation shows that May 13, 2015, storm is a product of two substorms. A remarkable increase in TEC is observed mainly during the daytime hours. A TEC peak of 75.38 TECU is observed at 1500 UT which is a maximum variation of 18.74 TECU. The B_Z variation on this day shows a succession of north and south direction of the IMF during the main phase and the recovery phase of the storm. During this time, a succession of eastern and western direction of IEF is observed. Due to the fact that the B_Z and Ey oscillate significantly does not give a clear direction of IMF and IEF, so PPEF cannot be the cause of the increase in the TEC during these hours. However, a strong increment in solar wind proton pressure and temperature is observed between 2300 UT (May 12) and 0800 UT (May 13), which corresponds to the storm main phase. Therefore, this increase could be due to the dynamic pressure of the solar wind or the effect of neutral winds in the thermosphere. Lissa et al. [58] studied the response of equatorial and low-latitude ionosphere during an intense geomagnetic storm on August 26, 2018, using TEC observations from chains of GPS stations, namely, Colombo, Bengaluru, Hyderabad, and Lucknow, and observed the storm positive effect during the main and recovery phases that attributed to the fast eastward-penetrating electric fields in addition to the strongly enhanced ratio of the neutral thermospheric composition. Also, the strong increase in TEC on May 13 between 1100 UT and 1500 UT may be associated with local electrodynamics or storm-induced meridional winds [54].

On May 14, 2015, first day after the storm, Dst index returns to the normal variation of a calm day but still negative with a first low value (-33nT) at 0500 UT and a second (-32nT) at 1600 UT. This characterizes the substorm signature. The TEC increased sharply mainly during the daytime hours with a peak of 78.12 TECU at 1400 UT, either an increment of 21.51 TECU. However, the B_Z is north-facing and the IEF Ey is west-facing. Also, low values of solar wind temperature and pressure compared to the day of the storm are observed. Thus, it is clear that this TEC enhancement is neither associated with the PPEF nor with the dynamic solar wind pressure. These enhancements could be due to the storm-induced neutral wind effect. This phenomenon may result from the superposition of two substorms successive indicated by two successive southward Dst perturbations. These results are consistent with the results reported by Jin et al. [29] for the March 2015 geomagnetic storm. May 15, 2015, is marked by a positive TEC of 17.34 TECU. During this time the B_Z is oriented to the south and Ey to the east. Therefore, the possible cause of this increase could be the effect of the PP electric field.

3.2. TEC Variation from September 09 to September 13, 2015. Variation of Dst index, solar wind speed (SSW), proton pressure (SWP), solar wind proton temperature (SWPT), horizontal component of the interplanetary magnetic field (IMF B_Z), component y of the interplanetary electric field (IEF Ey), and total electron content (TEC) at the Koudougou station from September 09 to 13, 2015, are presented in Figures 3(a)–3(f), respectively. This moderate geomagnetic storm started on September 11, 2015, around 0200 UT with a southward orientation of Dst followed by a decrease in its values where it reaches its minimum (-81 nT) that same day at 1500 UT. The geomagnetic storm of September 9-13, 2015, is actually a combination of three successive minima of Dst, the first of which (-70 nT) arrived on September 7, 2015, followed by a period of rapid recovery. The second departure of Dst occurred on September 9, 2015, with the lowest level of -98 nT around 1300 UT [59]. The third excursion of the lowest Dst value (-81 nT at 1500 UT) is observed on September 11, 2015, after a long recovery phase (about 48 hours) from the previous substorm.

The variation of TEC on 09 September 2015 is less than regular variation on calm days between 0000 UT and 1100 UT. This is despite a southern orientation of B_Z and an eastern orientation of IEF Ey, respectively, during these hours. According to Fejer [55], Huang et al. [56], and Singh et al. [54], when the IMF B_Z is south oriented and the dawn-dusk component of interplanetary electric field (IEF) Ey computed by Zhao et al. [60] is east oriented, a probable increase in TEC is expected. This is not the case here. It is noticed that solar wind speed is low (less than 450 km/s), as well as solar wind temperature, but a weak oscillation of solar wind pressure is noted from 0000 UT to 1300 UT. The possible cause of this TEC depression could be the slow decay rate of ring current observed during the main phase of this storm shown by the Dst index. After the negative variation, a positive TEC with a very small increase (2 TECU) is observed between 1200 UT and 1500 UT. This corresponds to periods of intense sunshine at the Koudougou station. Since the PP electric field is in the same direction as the ambient electric field (IEF Ey towards the east), it pushes up the $E \times B$ drift towards higher altitudes [61]. Due to the larger production/loss ratio at higher altitudes, the TEC increases during sunlight hours (B. [62]). Reddybattula et al. [49] had also found a positive TEC during the main phase of September 09, 2015, storm over the Indian region. The TEC becomes negative again from 1700 UT to 0500 UT of September 10. This period corresponds to the night hours at the Koudougou station. Since at night, the PP electric field and the ambient field are of opposite polarity [54], which could be the cause of this depression.

September 10, 2015, located on the recovery phase of September 09 storm, has a higher TEC peak than the day of September 09 and 10. The TEC is negative during the night hours (0100 to 0500 UT and 1900 to 2300 UT) and during hours of low sunshine (0600 to 0900 UT) and positive during hours of high sunshine (between 1000 and 1700 UT) at the Koudougou station. During the whole day of September 10, B_Z and Ey oscillate between positive and negative values. This does not give a clear direction of IMF

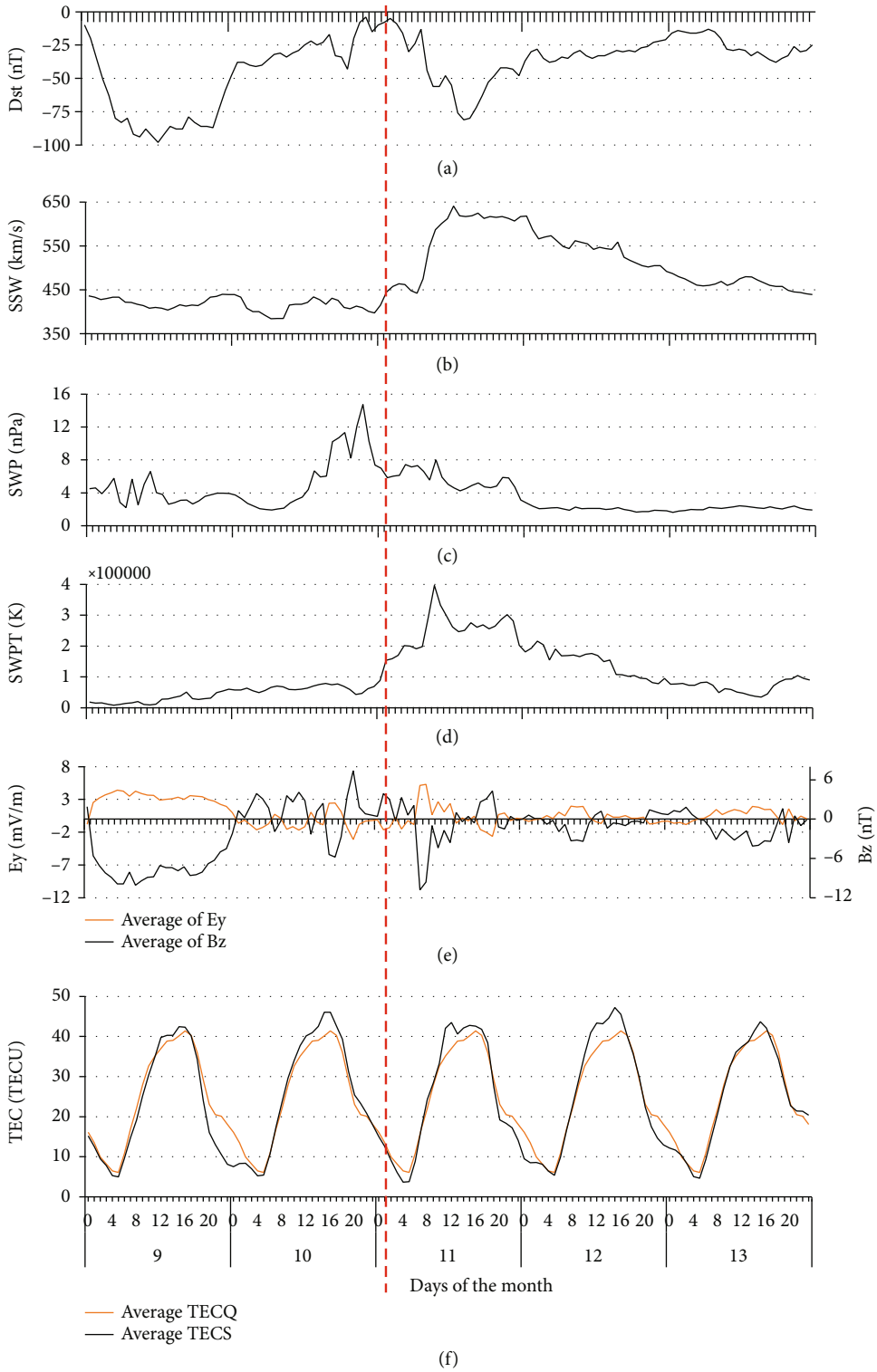

Figure 3: Variation of solar wind parameters and total electron content (TEC) from September 09 to 13, 2015, at the Koudougou GPS station.

and IEF. An increment of 5.88 TECU is observed 1500 UT. This increase could be due to the effect of the wind induced by September 09 storm.

Dst variation shows a southward orientation where its lowest value (-81 nT) is observed on September 11, 2015, at 1400 UT. This characterizes the presence of a new storm. TEC is negative during the night hours and positive only between 1100 and 1700 UT; however, the variation remains small (less than 2 TECU) except between 1100 and 1200 UT where it is worth 6 TECU. During this time, B_Z component

has shifted southward with a decrease of 12.7 nT (2.1 nT to -10.8 nT), and the IEF Ey shows an eastward orientation from 0700 to 1300 UT. Indeed, the increase in the TEC observed between 1100 and 1700 UT may be associated with the PP electric field caused by the direct and rapid penetration of electric field at dawn [63]. The onset of September 11 storm is also marked by an increased growth of solar wind speed and proton temperature. However, a decrease in pressure is observed. This could also justify the TEC increase by the Joule heating effect of thermospheric neutral winds. The low pressure rate of solar wind dynamics could be the cause of the small variation of TEC observed.

From 1600 UT on September 11, Dst index started to turn northward and reached its calm day background level at 1900 UT on September 12. Thus, the storm is in its recovery phase. As on previous days, the TEC is positive during the daytime hours and negative during the nighttime hours but with a peak (47.21 TECU) higher than on September 11 (42.56 TECU). However, B_Z shows fluctuations, sometimes southward, sometimes northward. IEF Ey undergoes the same orientation variation but from east-west. The effect of neutral wind induced by storm could play on this increase. On September 13, 2015, the TEC curve is almost confused with the curve of the regular variation of calm days except between 1300 and 1600 UT that a notable difference is observed.

In general, May TEC values at the Koudougou GPS station are higher than those of September. This difference could be justified by the seasonal influence on variation of TEC [64]. During the study of these two events (storm of 11-15 May 2015 and storm of 09-13 September 2015) at the Koudougou station, it is found that when Dst index turns southward at the beginning of storm without changing sign, the TEC peak of day following storm is always higher than that of storm day. At the Koudougou station, the difference varies between 2 and 5 TECU depending on the storm. This shows the important contribution of the winds induced by storms on the variation of TEC, since these moments are much more influenced by these winds.

3.3. TEC Variation from June 06 to June 10, 2015. Variation of Dst index, solar wind speed (SSW), proton pressure (SWP), solar wind proton temperature (SWPT), horizontal component of interplanetary magnetic field (IMF B_Z), component y of interplanetary electric field (IEF Ey), and total electron content (TEC) at the Koudougou station from June 06 to 10, 2015, are presented in Figures 4(a)–4(f), respectively. Figure 4(a) shows that Dst index started to turn southward at 0300 UT on 08 June 2015 and reached the lowest value of -73 nT at 0800 UT. It is also observed that IMF B_Z turned south at 0400 UT and remained in this direction until 0800 UT when it reached a value of -14.6 nT. At the same time, IEF Ey values ranged from -1.63 to 6.74 mV/m (8.37 mV/m increment). Subsequently, IMF B_Z turned south again at 1400 UT and reached the lowest value of magnitude -5.6 nT. It remained southward until 1700 UT on June 08. Meanwhile, IEF Ey turned eastward and changed from 3.78 mV/m (-0.13) to 3.65 mV/m. The rapid upward and downward changes in IMF B_Z show the presence of a sudden storm commencement (SSC) [54]. This is not the case here as no SSC was reported on this day on the International Service of Geomagnetic Indices (ISGI) site. This shows that gradual onset storms can also have rapid recursions on IMF B_Z. The storm main phase is marked by a rapid increase in solar wind parameters.

The Dst variation shows that 06 and 07 June 2015 are very calm geomagnetic days with Dst turned northward and of positive values. Despite this, a positive TEC is observed during these days mainly during the daytime hours. However, the exact mechanism responsible for the increase in ionospheric electron density prior to the storm is still a matter of debate [65, 66]. The TEC amplitude on 07 June is larger than that on 06 June, and the cause could not be the effect of PP electric field because the B_Z magnetic field faces north and the IEF Ey faces west from 0800 UT to 1900 UT on 07 June 2015.

The TEC variation is positive all day on June 08, 2015, at the Koudougou station, even during the night hours. Nevertheless, it is during the daytime hours that a strong increase is observed, i.e., a magnitude of 15.13 TECU at 1400 UT. During this day, Dst is facing south; IMF B_Z is facing south from 0400 to 0800 UT and then from 1200 UT to 1700 UT. At this time, IEF Ey is facing east. These indications show that the increase in TEC could be associated with the convection electric field in the magnetosphere described as the primary source of the PP electric field [54]. The high peak in the TEC on this day could also be the contribution of effect heating caused by the high solar wind temperature or the high solar wind dynamic pressure, since an enhanced growth of solar wind parameters is observed. The increase of TEC during the storm of 08 June 2015 at the station of Koudougou is evaluated at 34.43%, and that of the day before and after the storm is evaluated, respectively, at 16.84% and 26.82%.

On 08 June around 1800 UT, the Dst index started to turn northward and reached its calm day background level at 0800 UT on 09 June 2015. Thus, a long recovery phase was maintained for the 08 June 2015 storm. However, a transient behavior of Dst index is observed during the recovery phase where it showed twice a south polarity, the first at 1800 UT on June 09 (-42 nT) and the second at 1500 UT on June 10 (-31 nT). The north-south oscillation of IMF B_Z and Dst index is associated with an increase of solar wind speed which reaches 650 km/s at 1800 UT on June 10. This shows the low intensity substorm condition of 09-10 June 2015. These substorm processes could be associated with the increases in TEC amplitudes observed over almost the entire period [57]. The large increases in TEC observed from 09-10 June during daylight hours may be due to the effect of neutral wind induced by the 08 June storm.

3.4. TEC Variation from May 06 to May 11, 2016. Variation of Dst index, solar wind speed (SSW), proton pressure (SWP), solar wind proton temperature (SWPT), horizontal component of interplanetary magnetic field (IMF B_Z), component y of interplanetary electric field (IEF Ey), and total electron content (TEC) at the Koudougou station from May 06 to 11, 2016, are presented in Figures 5(a)–5(f),

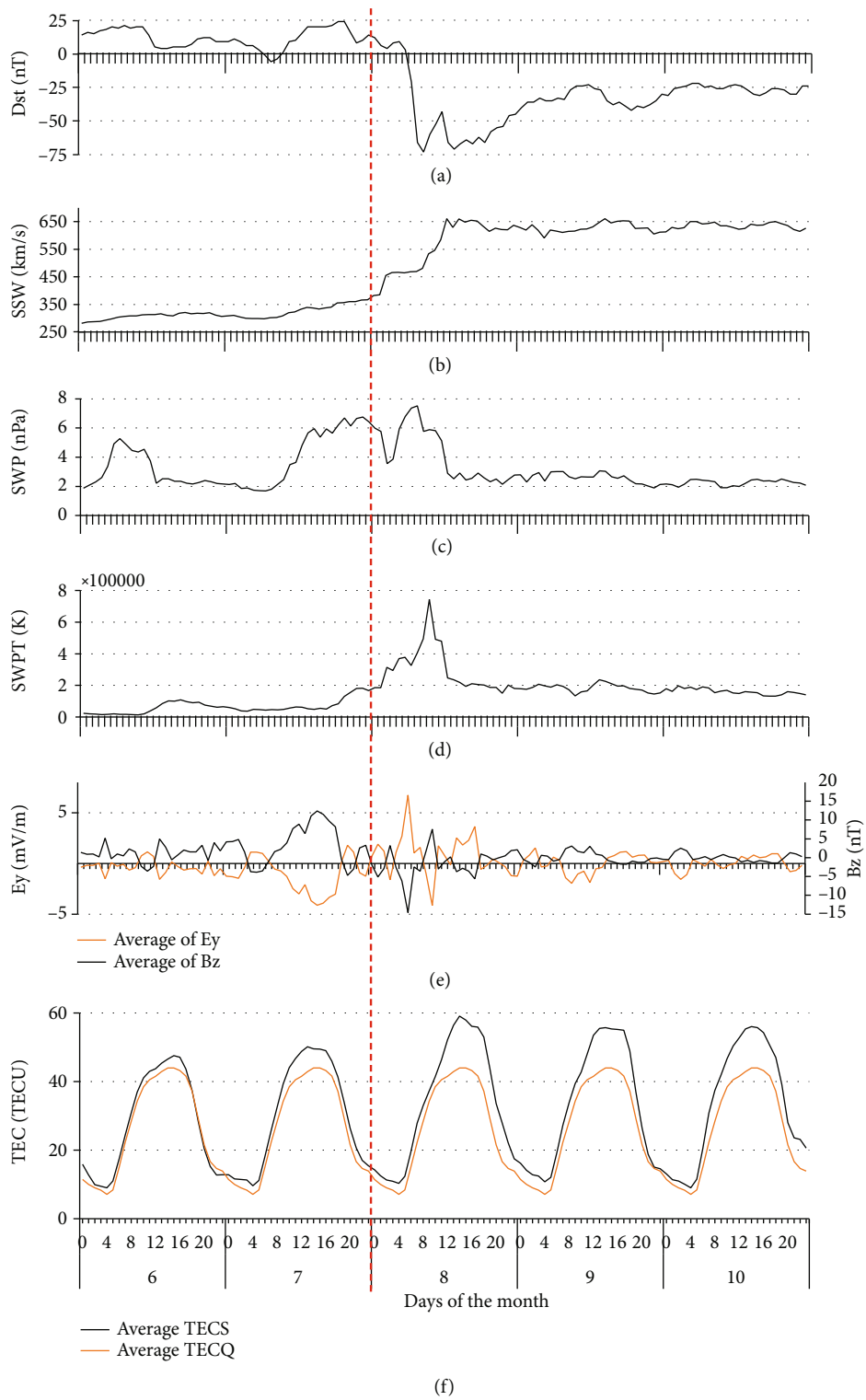

Figure 4: Variation of solar wind parameters and total electron content (TEC) from June 06 to 10, 2015, at the Koudougou GPS station.

respectively. It is clear from Figure 5 that the geomagnetic storm main phase of 08-09 May 2016 started at 0000 UT on 08 May and ended at 0000 UT on 09 May 2016 where it reached the lowest Dst value of -88 nT on 08 May at 0800 UT. After that, the recovery phase started on 09 May around 0100 UT, and Dst values returned to the calm day background level on 10 May at 1600 UT. Similarly, the variation of IMF B_Z shows that it started to turn southward along with the Dst and reached the lowest values of -11.4 nT at 0200 UT. On 08 June at 0800 UT, the IMF B_Z also turned northward but remained in a negative phase until 1400 UT when it again returned to the south direction until

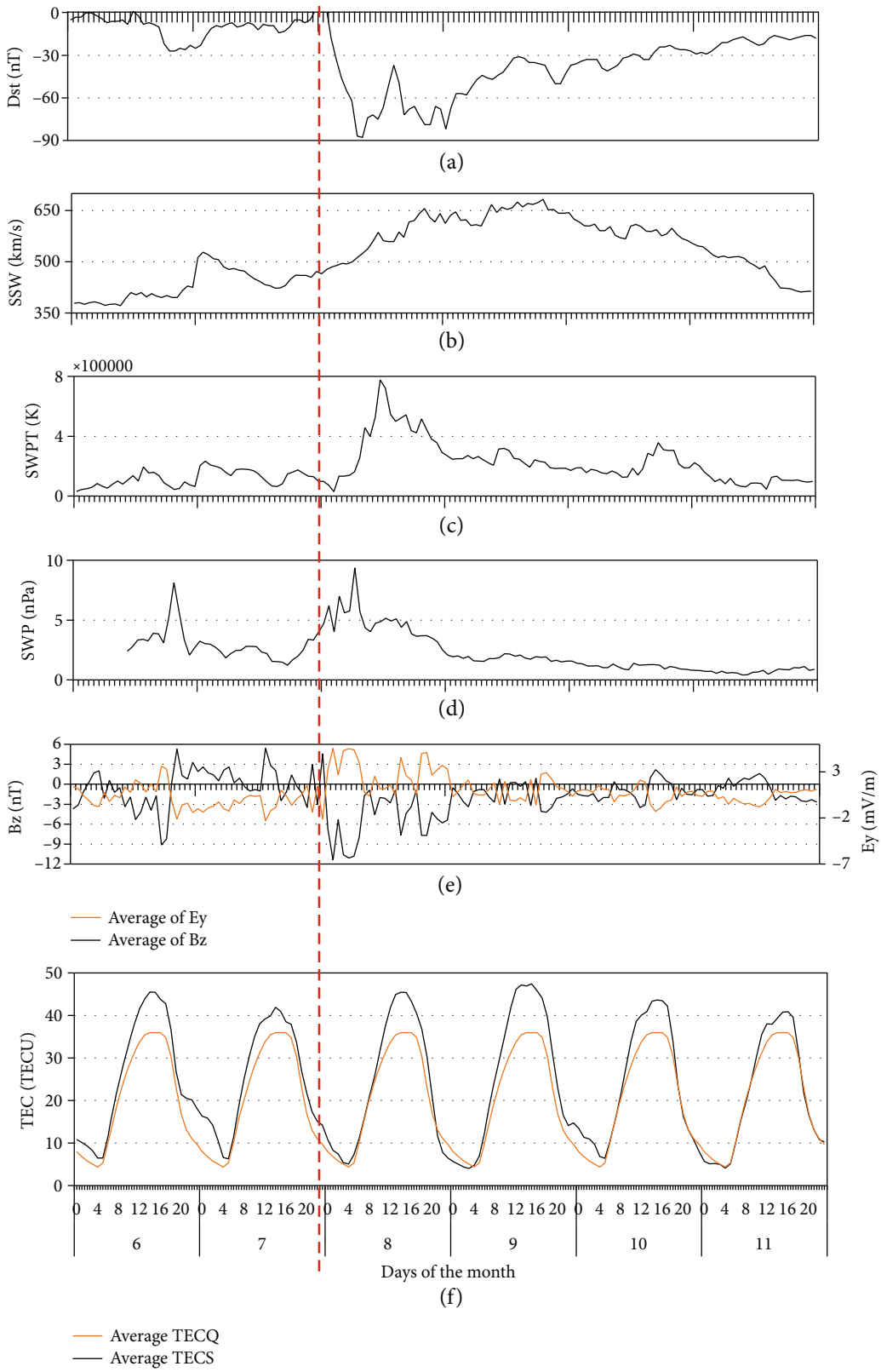

Figure 5: Variation of solar wind parameters and total electron content (TEC) from May 06 to 11, 2016, at the Koudougou GPS station.

09 May at 0200 UT. The variation of IEF Ey shows that it was in exactly the opposite phase of IMF B_Z. It was directed to the east, and its value increased significantly by 7.72 mV/m (-02.14 to 5.58). The variation of TEC shows an increase between 0800 and 1400 UT of 9.52 TECU on May 08 and an increase of 11.71 TECU on May 09, 2016, an increase of

26.47% and 33.05%, respectively, from the level of quiet day. The increase in TEC was likely associated with the PP electric field as confirmed by the change in IEF Ey value during the increase in TEC values. However, a time interval of 3 to 4 hours is required to observe any disturbance in the vertical drift of IEF [61].

Before the event of 08-09 May 2016, a rise in solar wind speed values is observed on 07 May at 0200 UT where it reached 521 km/s. But well before this date, a peak of 8.14 nPa is observed in SWP values on 06 May at 1900 UT. During this time, the B_Z is turned southward between 1100 and 1800 UT, but the variation of IEF Ey shows a westward orientation except at 1800 UT where it is directed eastward. These observed characteristics could be the condition of passage of a fast solar wind. All day on May 07, the IEF Ey was facing west and the IMF B_Z and the Dst are oriented to the north. This could justify the low amplitude of TEC observed this day. Indeed, if the IMF B_Z is northward, there is no reconnection between the IMF and the Earth's magnetic field during the day. The discontinuity of SWP curve between 0000 and 0600 UT on May 06 is due to the lack of data recorded in the OMNIWeb database.

On May 10 and 11, 2016, TEC shows positive variation from the quiet day especially during the daytime hours but with a small amplitude compared to those of 08-09 May. During these two days, IEF Ey is almost westward with no polarity inversion and IMF B_Z is northward with a southward direction on May 10 from 1400 to 1700 UT and on May 11 from 1000 to 1300 UT. However, the likely cause of the increased TEC on these days is the effect of storm-induced neutral winds.

The global study of events of 08 June 2015 and 08-09 May 2016 shows an almost identical behavior of TEC. Indeed, during these storms, TEC is positive during almost the whole day but weak during the night hours. The Dst shifts to the north direction at storm beginning before turning south during the main phase. The observation is that the TEC amplitude on the day of storm is greater than on the day after storm. The opposite effect is observed at the May 13 and September 11, 2015, storms. Thus, this behavior of TEC can be explained by the behavior of Dst index.

4. Conclusions

We examined solar wind parameters' roles in the formation of a few selected recurrent type moderate geomagnetic storms during the solar cycle 24 descending phase and the response of equatorial GPS-TEC at the Koudougou station to these storms. All of the moderate geomagnetic storms studied were found to be associated with manifestations of fast solar winds (**SSW ≥ 500 km/s**). These storms are unique in terms of the Dst index behavior prior to the onset of event (negative in May 13 and September 11, 2015, storms and positive in June 08, 2015, and May 08-09, 2016, storms). Our results show TEC increase as a function of geomagnetic parameter (magnitude and polarity) variation and local weather at the Koudougou station, and TEC slightly decreases during the September 11, 2015, storm at a few hours of the day over the period of September 09-13, 2015. The results of this work also show that the storm-induced electric field and neutral winds are the main drivers of observed TEC changes during the selected geomagnetic storms. However, some differences were observed in the behavior of TEC as a function of variation of Dst: (1) when the Dst goes through positive values (north direction) before reversing to negative values (south direction) at the storm beginning, the IMF is southward and the solar wind pressure is increased during the main phase of storm. And the TEC amplitude observed on storm day is higher than that on the days before and after the storm. (2) But when the Dst passes to the south direction without sign change at storm beginning, IMF B_Z and IEF Ey oscillate without a specific direction during the main of storm. At this time, the TEC peak during the storm is small compared to the days before and after the storm. The physical phenomenon associated with such TEC behavior is not revealed, but future studies will justify this. Of all the geomagnetic storms considered, the positive ionospheric TEC effect was more pronounced during the June 08, 2015, event and much less pronounced during the September 11 event. Specifically, a moderate geomagnetic storm of recurrent type increases the maximum TEC at the Koudougou station by about 2-21 TECU.

This study provides an overview of the origins and progression of moderate recurrent geomagnetic storms and their impacts on the total electron content (TEC) of the ionosphere at the Koudougou station, an equatorial station located in West African region; this will help to develop mechanisms for predicting the response of African equatorial TEC to different geomagnetic storms.

Data Availability

The total electron content (TEC) data used to support the findings of this study are included within the supplementary information file(s). The solar wind parameter (speed, pressure, and temperature) data used are available at the OMNIWeb site (https://omniweb.gsfc.nasa.gov/form/dx1.html). The Bz component and B scalar of the interplanetary magnetic field data used are available at the OMNIWeb site (https://omniweb.gsfc.nasa.gov/form/dx1.html). The geomagnetic index (Dst) data used are available at the ISGI site (http://isgi.unistra.fr/data_download.php). The geomagnetic index (Kp) data used are available at the OMNIWeb site (https://omniweb.gsfc.nasa.gov/form/dx1.html). The solar sunspot number index data used are available at the SILSO site (https://www.sidc.be/silso/datafiles).

Conflicts of Interest

The authors have not declared any conflict of interests.

Acknowledgments

The authors thank ISGI and OMNIWeb for making the data used in this article available. This study is financed by the authors' own funds.

References

[1] G. Siscoe and R. Schwenn, "CME disturbance forecasting," *Space science reviews*, vol. 123, no. 1-3, pp. 453–470, 2006.

[2] A. Singh, D. Siingh, and R. Singh, "Space weather: physics, effects and predictability," *Surveys in Geophysics*, vol. 31, no. 6, pp. 581–638, 2010.

[3] K. Patel, A. Singh, S. Singh, and A. Singh, "Causes responsible for intense and severe storms during the declining phase of solar cycle 24," *Journal of Astrophysics and Astronomy*, vol. 40, no. 1, pp. 1–9, 2019.

[4] V. Bothmer and R. Schwenn, "The interplanetary and solar causes of major geomagnetic storms," *Journal of Geomagnetism and Geoelectricity*, vol. 47, no. 11, pp. 1127–1132, 1995.

[5] N. Gopalswamy, S. Yashiro, and S. Akiyama, "Geoeffectiveness of halo coronal mass ejections," *Journal of Geophysical Research: Space Physics*, vol. 112, no. A6, 2007.

[6] Y. Kamide, N. Yokoyama, W. Gonzalez et al., "Two-step development of geomagnetic storms," *Journal of Geophysical Research: Space Physics*, vol. 103, no. A4, pp. 6917–6921, 1998.

[7] N. Crooker and E. Cliver, "Postmodern view of M-regions," *Journal of Geophysical Research: Space Physics*, vol. 99, no. A12, pp. 23383–23390, 1994.

[8] B. T. Tsurutani, W. D. Gonzalez, A. L. Gonzalez, F. Tang, J. K. Arballo, and M. Okada, "Interplanetary origin of geomagnetic activity in the declining phase of the solar cycle," *Journal of Geophysical Research: Space Physics*, vol. 100, no. A11, pp. 21717–21733, 1995.

[9] J. Zhang, I. Richardson, D. Webb et al., "Solar and interplanetary sources of major geomagnetic storms (Dst≤−100 nT) during 1996–2005," *Journal of Geophysical Research: Space Physics*, vol. 112, no. A10, 2007.

[10] P. Perreault and S. Akasofu, "A study of geomagnetic storms," *Geophysical Journal International*, vol. 54, no. 3, pp. 547–573, 1978.

[11] A. Akala, E. Somoye, and A. Adeloye, "The response of African equatorial foF2 to geomagnetic storms: comparison between observations and IRI-2007 predictions," *Advances in Space Research*, vol. 45, no. 10, pp. 1211–1218, 2010.

[12] A. Dessler and E. N. Parker, "Hydromagnetic theory of geomagnetic storms," *Journal of Geophysical Research*, vol. 64, no. 12, pp. 2239–2252, 1959.

[13] N. Sckopke, "A general relation between the energy of trapped particles and the disturbance field near the Earth," *Journal of Geophysical Research*, vol. 71, no. 13, pp. 3125–3130, 1966.

[14] W. D. Gonzalez and B. T. Tsurutani, "Criteria of interplanetary parameters causing intense magnetic storms (Dst<−100 nT)," *Planetary and Space Science*, vol. 35, no. 9, pp. 1101–1109, 1987.

[15] B. T. Tsurutani, W. D. Gonzalez, F. Tang, S. I. Akasofu, and E. J. Smith, "Origin of interplanetary southward magnetic fields responsible for major magnetic storms near solar maximum (1978–1979)," *Journal of Geophysical Research: Space Physics*, vol. 93, no. A8, pp. 8519–8531, 1988.

[16] W. Gonzalez, J.-A. Joselyn, Y. Kamide et al., "What is a geomagnetic storm?," *Journal of Geophysical Research: Space Physics*, vol. 99, no. A4, pp. 5771–5792, 1994.

[17] C. Loewe and G. Prölss, "Classification and mean behavior of magnetic storms," *Journal of Geophysical Research: Space Physics*, vol. 102, no. A7, pp. 14209–14213, 1997.

[18] L. Burlaga and K. Ogilvie, "Causes of sudden commencements and sudden impulses," *Journal of Geophysical Research*, vol. 74, no. 11, pp. 2815–2825, 1969.

[19] C. O. Hines and L. Storey, "Time constants in the geomagnetic storm effect," *Journal of Geophysical Research*, vol. 63, no. 4, pp. 671–682, 1958.

[20] P. Mayaud, "The annual and daily variations of the Dst index," *Geophysical Journal International*, vol. 55, no. 1, pp. 193–201, 1978.

[21] H. Nevanlinna and E. Kataja, "An extension of the geomagnetic activity index seriesaafor two solar cycles (1844-1868)," *Geophysical Research Letters*, vol. 20, no. 23, pp. 2703–2706, 1993.

[22] S. Vennerstroem, "Long-term rise in geomagnetic activity–a close connection between quiet days and storms," *Geophysical Research Letters*, vol. 27, no. 1, pp. 69–72, 2000.

[23] J. Legrand and P. Simon, "Solar cycle and geomagnetic activity: a review for geophysicists. Part I. The contributions to geomagnetic activity," *Annales Geophysicae*, vol. 7, no. 6, pp. 565–578, 1989.

[24] F. Ouattara and C. Amory-Mazaudier, "Solar-geomagnetic activity and Aa indices toward a standard classification," *Journal of Atmospheric and Solar-Terrestrial Physics*, vol. 71, no. 17-18, pp. 1736–1748, 2009.

[25] J.-L. Zerbo, C. Amory Mazaudier, F. Ouattara, and J. Richardson, "Solar wind and geomagnetism: toward a standard classification of geomagnetic activity from 1868 to 2009," *Annales Geophysicae*, vol. 30, no. 2, pp. 421–426, 2012.

[26] A. Akala, G. Seemala, P. Doherty et al., "Comparison of equatorial GPS-TEC observations over an African station and an American station during the minimum and ascending phases of solar cycle 24," *Annales Geophysicae*, vol. 31, no. 11, pp. 2085–2096, 2013.

[27] A. Calabia, C. Anoruo, M. Shah et al., "Low-latitude ionospheric responses and coupling to the February 2014 multiphase geomagnetic storm from GNSS, magnetometers, and space weather data," *Atmosphere*, vol. 13, no. 4, p. 518, 2022.

[28] A. Calabia and S. Jin, "Thermospheric mass density disturbances due to magnetospheric forcing from 2014–2020 CASSIOPE precise orbits," *Journal of Geophysical Research: Space Physics*, vol. 126, no. 8, article e2021JA029540, 2021.

[29] S. Jin, R. Jin, and H. Kutoglu, "Positive and negative ionospheric responses to the March 2015 geomagnetic storm from BDS observations," *Journal of Geodesy*, vol. 91, no. 6, pp. 613–626, 2017.

[30] J. Joselyn and P. McIntosh, "Disappearing solar filaments: a useful predictor of geomagnetic activity," *Journal of Geophysical Research: Space Physics*, vol. 86, no. A6, pp. 4555–4564, 1981.

[31] P. Galav, N. Dashora, S. Sharma, and R. Pandey, "Characterization of low latitude GPS-TEC during very low solar activity phase," *Journal of Atmospheric and Solar-Terrestrial Physics*, vol. 72, no. 17, pp. 1309–1317, 2010.

[32] J. A. Klobuchar, "Ionospheric time-delay algorithm for single-frequency GPS users," *IEEE Transactions on Aerospace and Electronic Systems*, vol. AES-23, no. 3, pp. 325–331, 1987.

[33] J. Huba, G. Joyce, and J. Fedder, "Sami2 is another model of the ionosphere (SAMI2): a new low-latitude ionosphere model," *Journal of Geophysical Research: Space Physics*, vol. 105, no. A10, pp. 23035–23053, 2000.

[34] M. M. Hoque, N. Jakowski, and J. Berdermann, "Ionospheric correction using NTCM driven by GPS Klobuchar coefficients for GNSS applications," *GPS Solutions*, vol. 21, no. 4, pp. 1563–1572, 2017.

[35] D. Okoh, S. Onwuneme, G. Seemala et al., "Assessment of the NeQuick-2 and IRI-Plas 2017 models using global and long-term GNSS measurements," *Journal of Atmospheric and Solar-Terrestrial Physics*, vol. 170, pp. 1–10, 2018.

[36] S. M. Radicella, "The NeQuick model genesis, uses and evolution," *Annals of Geophysics*, vol. 52, no. 3-4, pp. 417–422, 2009.

[37] D. Bilitza, "IRI the international standard for the ionosphere," *Advances in Radio Science*, vol. 16, pp. 1–11, 2018.

[38] F. Ding, W. Wan, B. Ning et al., "Observations of poleward-propagating large-scale traveling ionospheric disturbances in southern China," *Annales Geophysicae*, vol. 31, no. 2, pp. 377–385, 2013.

[39] M. Piersanti, T. Alberti, A. Bemporad et al., "Comprehensive analysis of the geoeffective solar event of 21 June 2015: effects on the magnetosphere, plasmasphere, and ionosphere systems," *Solar Physics*, vol. 292, no. 11, pp. 1–56, 2017.

[40] M. Chakraborty, S. Kumar, B. K. De, and A. Guha, "Effects of geomagnetic storm on low latitude ionospheric total electron content: a case study from Indian sector," *Journal of Earth System Science*, vol. 124, no. 5, pp. 1115–1126, 2015.

[41] N. Dashora, S. Sharma, R. S. Dabas, S. Alex, and R. Pandey, "Large enhancements in low latitude total electron content during 15 May 2005 geomagnetic storm in Indian zone," *Annales Geophysicae*, vol. 27, no. 5, pp. 1803–1820, 2009.

[42] P. Galav, S. Sharma, S. S. Rao, B. Veenadhari, T. Nagatsuma, and R. Pandey, "Study of simultaneous presence of DD and PP electric fields during the geomagnetic storm of November 7–8, 2004 and resultant TEC variation over the Indian region," *Astrophysics and Space Science*, vol. 350, no. 2, pp. 459–469, 2014.

[43] S. Kumar and A. K. Singh, "GPS derived ionospheric TEC response to geomagnetic storm on 24 August 2005 at Indian low latitude stations," *Advances in Space Research*, vol. 47, no. 4, pp. 710–717, 2011.

[44] S. Kumar and A. K. Singh, "Storm time response of GPS-derived total electron content (TEC) during low solar active period at Indian low latitude station Varanasi," *Astrophysics and Space Science*, vol. 331, no. 2, pp. 447–458, 2011.

[45] N. M. Pedatella, J. Lei, K. M. Larson, and J. M. Forbes, "Observations of the ionospheric response to the 15 December 2006 geomagnetic storm: long-duration positive storm effect," *Journal of Geophysical Research: Space Physics*, vol. 114, no. A12, 2009.

[46] P. V. S. Rama Rao, S. Gopi Krishna, J. Vara Prasad, S. Prasad, D. Prasad, and K. Niranjan, "Geomagnetic storm effects on GPS based navigation," *Annales Geophysicae*, vol. 27, no. 5, pp. 2101–2110, 2009.

[47] S. Kumar, W. Chen, M. Chen, Z. Liu, and R. P. Singh, "Thunderstorm-/lightning-induced ionospheric perturbation: an observation from equatorial and low-latitude stations around Hong Kong," *Journal of Geophysical Research: Space Physics*, vol. 122, no. 8, pp. 9032–9044, 2017.

[48] A. Singh, V. Rathore, R. Singh, and A. Singh, "Source identification of moderate (-100 nT < Dst < -50 nT) and intense geomagnetic storms (Dst < -100 nT) during ascending phase of solar cycle 24," *Advances in Space Research*, vol. 59, no. 5, pp. 1209–1222, 2017.

[49] K. D. Reddybattula, S. K. Panda, K. Ansari, and V. S. R. Peddi, "Analysis of ionospheric TEC from GPS, GIM and global ionosphere models during moderate, strong, and extreme geomagnetic storms over Indian region," *Acta Astronautica*, vol. 161, pp. 283–292, 2019.

[50] F. Perira, *Analyse spatio-temporelle du champ géomagnétique et des processus d'accélération solaires observés en émission radio*, 2004.

[51] K. Kauristie, A. Morschhauser, N. Olsen et al., "On the usage of geomagnetic indices for data selection in internal field modelling," *Space Science Reviews*, vol. 206, no. 1-4, pp. 61–90, 2017.

[52] J. Matzka, C. Stolle, Y. Yamazaki, O. Bronkalla, and A. Morschhauser, "The GeomagneticKpIndex and derived indices of geomagnetic activity," *Space Weather*, vol. 19, no. 5, article e2020SW002641, 2021.

[53] S. A. Sandwidi and F. Ouattara, "Recurrent Events' Impacts on foF2 Diurnal Variations at Dakar Station during Solar Cycles 21-22," *International Journal of Geophysics*, vol. 2022, Article ID 4883155, 11 pages, 2022.

[54] A. Singh, V. S. Rathore, S. Kumar, S. S. Rao, S. K. Singh, and A. K. Singh, "Effect of intense geomagnetic storms on low-latitude TEC during the ascending phase of the solar cycle 24," *Journal of Astrophysics and Astronomy*, vol. 42, no. 2, p. 99, 2021.

[55] B. G. Fejer, C. A. Gonzales, D. T. Farley, M. C. Kelley, and R. F. Woodman, "Equatorial electric fields during magnetically disturbed conditions 1. The effect of the interplanetary magnetic field," *Journal of Geophysical Research: Space Physics*, vol. 84, no. A10, pp. 5797–5802, 1979.

[56] C.-S. Huang, S. Sazykin, J. L. Chau, N. Maruyama, and M. C. Kelley, "Penetration electric fields: efficiency and characteristic time scale," *Journal of Atmospheric and Solar-Terrestrial Physics*, vol. 69, no. 10-11, pp. 1135–1146, 2007.

[57] Y. Wei, Z. Pu, M. Hong et al., "Westward ionospheric electric field perturbations on the dayside associated with substorm processes," *Journal of Geophysical Research: Space Physics*, vol. 114, no. A12, 2009.

[58] D. Lissa, V. K. D. Srinivasu, D. Prasad, and K. Niranjan, "Ionospheric response to the 26 August 2018 geomagnetic storm using GPS-TEC observations along 80° E and 120° E longitudes in the Asian sector," *Advances in Space Research*, vol. 66, no. 6, pp. 1427–1440, 2020.

[59] S. Pérez-Plaza, F. Fernández-Palacín, M. Berrocoso, R. Páez, and B. Rosado, "Analysis of a gps network based on functional data analysis," *Mathematical Geosciences*, vol. 50, no. 6, pp. 659–677, 2018.

[60] B. Zhao, W. Wan, K. Tschu et al., "Ionosphere disturbances observed throughout Southeast Asia of the superstorm of 20–22 November 2003," *Journal of Geophysical Research: Space Physics*, vol. 113, no. A3, 2008.

[61] R. G. Rastogi and J. A. Klobuchar, "Ionospheric electron content within the equatorial F 2 layer anomaly belt," *Journal of Geophysical Research: Space Physics*, vol. 95, no. A11, pp. 19045–19052, 1990.

[62] B. Tsurutani, A. Mannucci, B. Iijima et al., "Global dayside ionospheric uplift and enhancement associated with interplanetary electric fields," *Journal of Geophysical Research: Space Physics*, vol. 109, no. A8, 2004.

[63] J. H. Sastri, K. B. Ramesh, and H. R. Rao, "Transient composite electric field disturbances near dip equator associated with

auroral substorms," *Geophysical Research Letters*, vol. 19, no. 14, pp. 1451–1454, 1992.

[64] L. Jose, S. Ravindran, C. Vineeth, T. K. Pant, and S. Alex, "Investigation of the response time of the equatorial ionosphere in context of the equatorial electrojet and equatorial ionization anomaly," *Annales Geophysicae*, vol. 29, no. 7, pp. 1267–1275, 2011.

[65] A. D. Danilov, "F2-region response to geomagnetic disturbances," *Journal of Atmospheric and Solar-Terrestrial Physics*, vol. 63, no. 5, pp. 441–449, 2001.

[66] L. Liu, W. Wan, M.-L. Zhang, B. Zhao, and B. Ning, "Prestorm enhancements in NmF2 and total electron content at low latitudes," *Journal of Geophysical Research: Space Physics*, vol. 113, no. A2, 2008.